

Triboelectrification of Single Crystals as a Function of Orientation and Surface Reconstruction

Adam L. Collins, Rhyan S.B. Ghosh, Seth J. Putterman
Dept. of Physics and Astronomy
University of California Los Angeles, Los Angeles, CA 90095

e-mail: alcollins@physics.ucla.edu

Abstract— Surfaces of materials are scarcely simple structural or electrical terminations of the bulk. Such reconstruction of the surface at the atomic level can provide significant changes to larger scale properties of the material (e.g. conductivity, phonon modes, work function, etc.). When considering triboelectrification, it is explicitly two surfaces that interact with each other. The structure of the surfaces can change from the original reconstructed shape, to a third combined structure at an *ad hoc* interface, before even considering the effects of larger scale stress and strain from the contact. Consideration for the effects of surface structural rearrangements on triboelectrification appears to have been overlooked. To investigate the effects of surface termination on triboelectrification, we present data on the contact charging of single crystal quartz and sapphire under vacuum conditions (< 1 mtorr). We choose single crystals to clarify material parameters at the atomic level, and perform measurements under vacuum to reduce environmental influence on the charging. We additionally monitor for triboluminescence (from RF up to X-ray energy) to account for any charge lost in discharge processes. Experiments are performed on four different sapphire crystal orientations (and hence terminations / reconstructions at the surface): C-plane (0001), A-plane (11-20), R-plane (1-102), and M-Plane (1-100). Each sapphire crystal is pressed against Z-cut quartz (0001), where triboelectrification is readily achieved.

I. INTRODUCTION

Triboelectrification (TE), the observed charging of initially neutral materials after being brought into and out of contact, has challenged scientists and philosophers since antiquity to explain a robustly observable phenomenon [1,2]. TE is the quintessential manifestation of surface effects over bulk material response such that atomic scale changes can be propagated to the macroscopic scale. It is remarkable that only recently have there been attempts to provide an *ab initio* theory of TE. [3,4]. Success has been limited, at best, in explaining TE at the *ab initio* level: the direction of charging still remains unpredictable, and even why charge should move at all between insulating surfaces remains an open question!

The failure to provide an *ab initio* theory for TE is at least in part due to the fact that the entire triboelectric process is off-equilibrium (as noted in [3-5]). The presence of triboluminescence (light emission following a triboelectric contact) explicitly demonstrates that charges are being rearranged in a non-reversible manner.

To bring triboelectrification as close as possible to *ab initio* theory, charge transfer between single-crystal unit cell materials is being studied with charge being tracked through the entire contact and separation process; i.e., discharges that occur on the way to residual charge are measured.

To construct an appropriate theory of triboelectrification, three aspects must be considered:

1. When contact is well-defined, triboelectrification is a repeatable phenomenon.[6,7] Triboelectricity is a multi-scale phenomenon, so both atomic / molecular and collective material properties matter.[8-10]
2. Surfaces and interfaces are not simple electrical or structural terminations of the bulk, so reconstructed surfaces must be considered.[11-16]

Apparatus was designed to take these considerations into account when making measurements [17].

TE must, at some level, result from a material parameter in order to retain its repeatability. Furthermore, since a TE interaction occurs explicitly between two surfaces, the key material property is likely a function of the surface structure – which is almost always different from the bulk.

If triboelectrification is a result of material properties derived from the surface structure, it will be important to define how that structure is different from the bulk, and how it may further reconstruct when in contact. Measurement and calculation of material surface structure and corresponding mechanical and electrical properties is an entire subject that will not be summarized here. However, progress can be made by simply acknowledging that the surface structure is different from the bulk, and that different crystal orientations can provide different surface structures for experiment. Accordingly, experiments are reported here for the triboelectrification of quartz (SiO_2 , z-cut, (0001)) pressed against four different sapphire (Al_2O_3) orientations: C-plane (0001), A-plane ($11\bar{2}0$), R-plane ($1\bar{1}02$), and M-Plane ($1\bar{1}00$). We seek to observe differences in charging behavior by surface orientation for the same bulk material.

II. EXPERIMENTAL ARRANGEMENT

A. Apparatus

A complete description of the apparatus can be found in reference [17], and a simplified schematic is shown in figure 1. Note that the anvils have been updated since reference [17] to be constructed of Teflon (PTFE) and Aluminum Silicate ($\text{Al}_2\text{Si}_4\text{O}_{10}(\text{OH})_2$) ceramic.

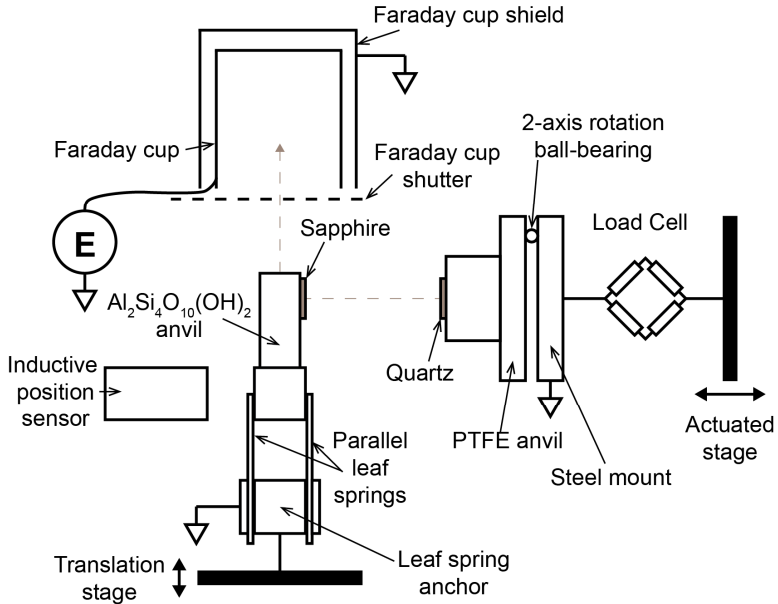


Fig. 1. Simplified schematic of the apparatus used in the experiments reported here, taken from [17]. The actuated stage moves a quartz crystal into a sapphire crystal, with the parallel leaf springs yielding to the contact and maintaining alignment. After contact and holding for a five seconds, the quartz is retracted, and the sapphire is moved into the Faraday cup with a translation stage. An X-ray detector, phototransistor, and RF antenna are not shown but are mounted to view from above, which is looking into the page in this diagram.

Over the course of an experiment, two aligned crystals are brought into and out of contact at 1 mm s^{-1} , during which the separation distance (inductive sensor), force (load cell), and triboluminescence (CdTe X-ray detector, RF antenna, and photodiode) are monitored. After contact and release, the sapphire crystal is slotted into a Faraday cup to measure the total residual charge on its surface, then returned to its original position. Experiments are performed under a vacuum of less than 10^{-3} Torr to take the system out of a traditional Paschen-type discharge regime [18] and reduce the influence of ambient gas on any discharge processes that may occur.

A typical experiment will press quartz and sapphire together to a force of 7 N, hold for 5 s, and then retract. A charging curve is generated by repeated contact of the crystals. If crystals have been previously charged, a tensile force is observed on the load cell as the crystals approach. By taking the measured Faraday cup charge from the prior contact (Q_F) and the magnitude of the tensile force just prior to the next contact (F_C), an approximation

can be made of the charged area (A) and density (σ) via equations 1 and 2 via a parallel plate capacitor assumption:

$$A = \frac{Q_F^2}{2\epsilon_0 F_C}; \quad (1)$$

$$\sigma = \frac{Q_F}{A} \quad (2)$$

where ϵ_0 is the permittivity of free space. The approximation assumes a homogenous charge distribution, with equal and opposite charges on each crystal.

If the charging becomes strong enough, electrostatic breakdown can occur between the crystals generating X-rays with a Bremsstrahlung spectrum given by the voltage between the crystals at the point of discharge.

B. Crystals

The structures of sapphire and quartz, with relevant planes highlighted, are shown in figure 2.

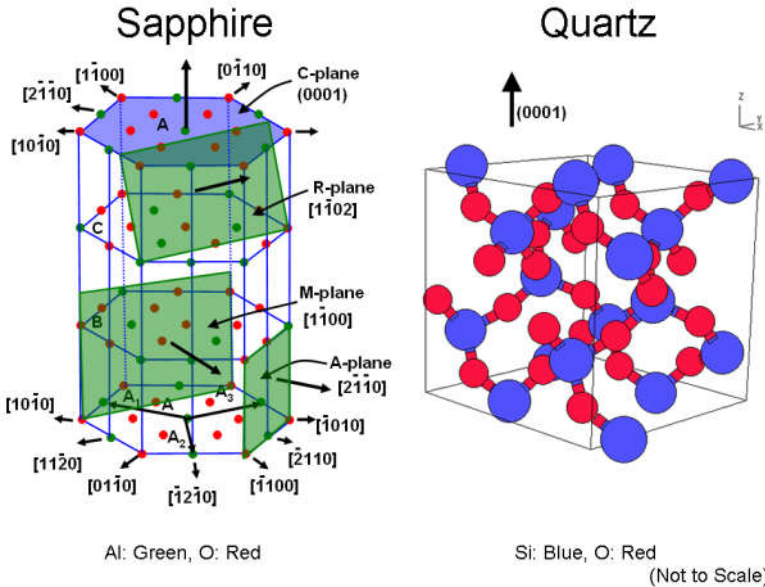


Fig. 2. Crystal structures of sapphire (left, edited from [19]) and quartz (right, edited from [20]). A-, C-, R-, and M-planes are defined for the sapphire structure, and the z-cut orientation (0001) for quartz is also shown. The planes are those used in experiments reported here.

Crystals were purchased from MTI Corporation (Richmond, CA), and cleaned *in situ* with high-purity acetone and a lint-free cloth. Some relevant properties of the crystals are shown in table 1. The crystals are polished by the manufacturer to have $R_a < 10 \text{ \AA}$.

TABLE 1: PROPERTIES OF SAPPHIRE AND QUARTZ SUPPLIED BY MANUFACTURER

| | Sapphire | Quartz |
|--------------------------------|--|---|
| Structure | Hexagonal | Hexagonal |
| Lattice Parameters | a = 4.758 Å c = 12.992 Å | a = 4.914 Å c = 5.405 Å |
| Hardness | 9 Moh's | 7 Moh's |
| Density | 3.980 g cm ⁻³ | 2.684 g cm ⁻³ |
| Relative Permittivity (@300 K) | 9.4 \hat{A} -direction 11.58 \hat{C} -direction | 4.43 \hat{x} -direction 4.63 \hat{z} -direction [21] |

III. RESULTS

Regardless of crystal orientation, sapphire consistently charged positively against quartz, in agreement with previously reported data for C-plane sapphire [3].

A typical set of charging curves for a pair of crystals is shown in figure 3, with inferred charge area and density in figure 4. Similar behavior is observed for all crystal orientations. The charge is seen to climb steadily to a few nC, and then plateau and slightly decay. The plateau is either indicative of crystals becoming misaligned during the experiment and hence losing contact quality or the charging becoming high enough to stimulate charge emission, leading to detectable X-rays (see figure 6).

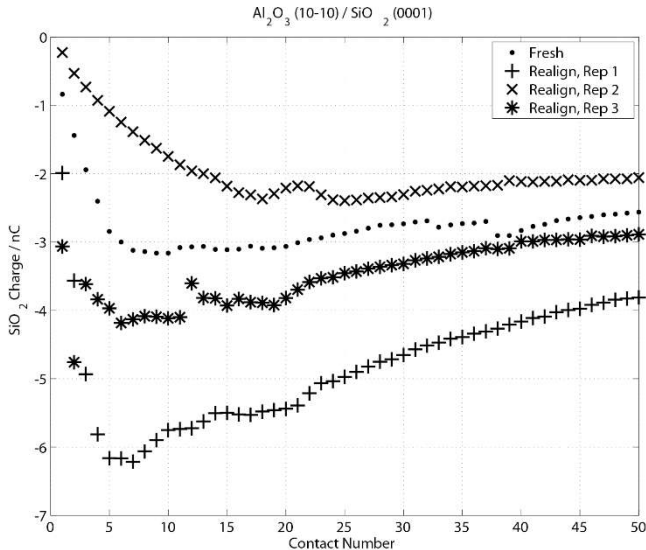


Fig. 3. Charging curve for quartz against M-plane oriented ($1\bar{1}00$) sapphire. This dataset is representative of typical of charging behavior seen by all crystal orientations against quartz. Quartz charges negatively, sapphire positively. Charging begins rapidly and rises over the first five contacts, and then either plateaus or slightly decays as contacts continue. The decay is attributed to loss of alignment during the experiment, or reaching a charging voltage threshold above which X-ray emission can occur.

Considering figure 4, the inferred charged area was variable across four repeats with the same crystals, though the charge density was less variable. The three datasets where the charged area was larger than 5% (indicative of good coverage) have settled to very similar charge densities, and it is asserted that this is indicative of a discharge threshold.

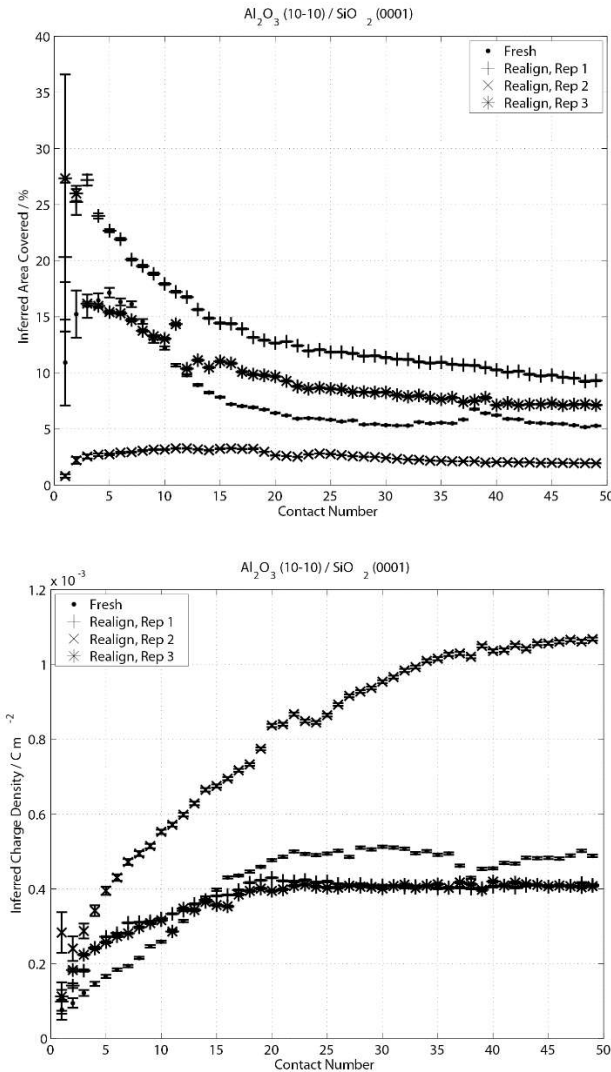


Fig. 4. Top: Inferred charged area (A) during contacts shown in figure 3. Bottom: Inferred charge density (σ). Despite a range of finite charging, there is some consistency to the charge density. The flattening of the charge density is attributed to the onset of X-ray discharge emission.

If the surface charge is assumed to be a disc of constant charge density with radius $\sqrt{\frac{A}{\pi}}$ on each crystal, and dielectric screening ignored, the voltage (V) between the disc centers at a distance z apart is given by equation 3 [10]:

$$V = \frac{\sigma}{2\epsilon_0} \sqrt{\frac{A}{\pi}} \left(1 + 2z \sqrt{\frac{\pi}{A}} - \sqrt{1 + \frac{4\pi z^2}{A}} \right). \quad (3)$$

Using the values from figure 4, and setting $z = 25.4 \text{ mm}$ (the separation of the crystals in their home position) the unscreened voltage is plotted in figure 5. Variation between the datasets of figures 3 and 4 has reduced with each set reaching a similar threshold voltage of $\sim 35\text{-}45 \text{ kV}$.

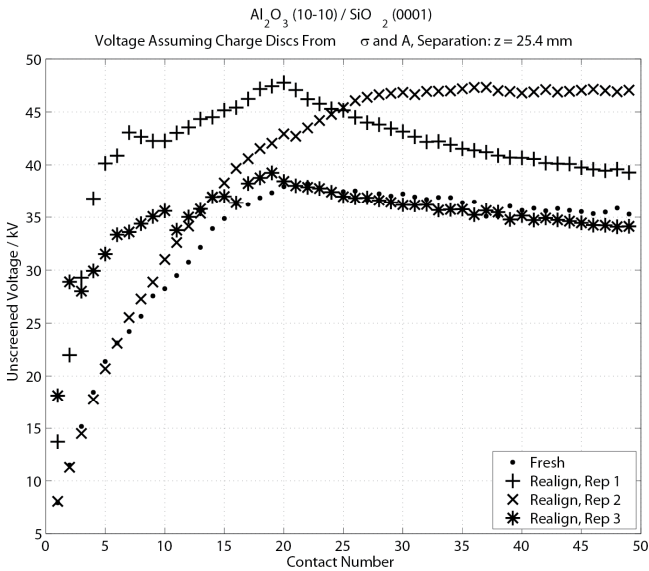


Fig. 5. “Unscreened” voltage between two oppositely charged discs with charge and extent derived from the values in figure 4 and processed through equation 3 ($z = 25.4 \text{ mm}$). The spread observed in figures 3 and 4 is reduced, suggesting that much of the charging is being limited by discharge at X-ray energies.

Figure 6 shows the loading curves for set “Realign, Rep 3” and detection of X-rays confirming the X-ray discharge implied by figure 5. Tensile force is negative, compressive is positive, and so the graph shows that as the crystals approach there is an attractive (tensile) force just prior to contact (as used in equations 1 and 2), at which point the force ramps up, clipping at 3 N (crystals are in fact loaded to 7 N). At pull-off there is some additional force of adhesion (sometimes substantially larger than pull-in), and the attractive electrostatic force steadily decays back to zero as the charged surfaces separate.

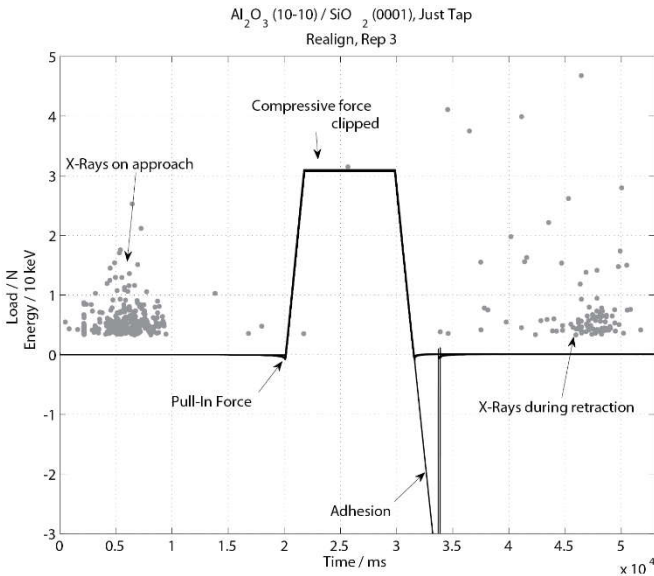


Fig. 6. Force/time profile for dataset “Realign, rep 3”, and associated X-ray detections. As crystals approach, if previously charged a tensile attractive force is observed (“pull-in force”) just prior to contact, followed by a more rapid rise as the crystals engage. On separation additional tensile force is observed, attributed to adhesion, followed by a more steady decay back to zero. Individual X-rays are observed during retraction of the crystals, and on re-approach suggesting the charge on the surfaces is quite stable.

In figure 7 is shown more closely how the force decays during separation for a different pair of crystals; on one particular instance there is an abrupt jump in force back to zero. The jump to zero is correlated with a substantial drop in measured charge, as well as a simultaneously occurring pulse of X-rays. All signs of an abrupt discharge event that can sometimes occur [7,17] rather than the steady decay of charge shown by the single X-ray detections of figure 6.

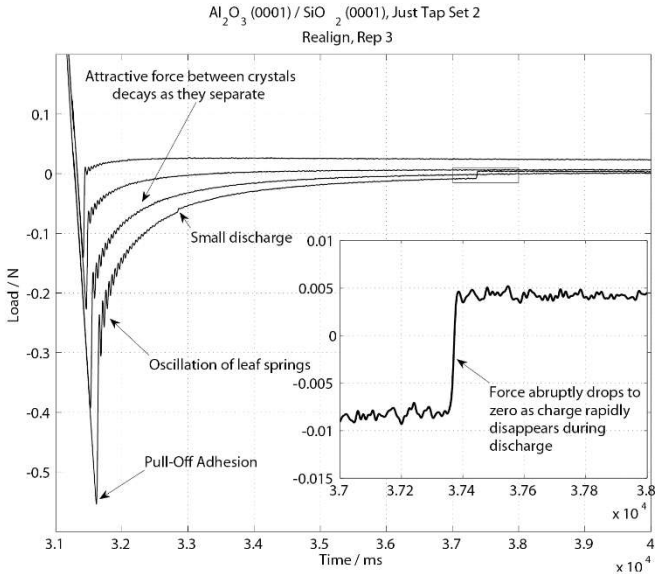


Fig. 7. Load cell output as C-plane sapphire separates from z-cut quartz at 1 mm/s. Following the adhesive force at pull-off, the force oscillates as the leaf springs unload, and the overall force steadily reduces in magnitude as the crystals separate. The tensile (negative) force exists as the oppositely charged crystals attract each other less and less as they get further apart. On one unloading curve, two abrupt jumps in the force are seen – these are attributed to large scale discharges of the surface, with the inset graph showing the almost total loss of force and hence charge from the surfaces. Such an abrupt discharge was accompanied by a flash of X-rays as the released charge collided with the opposing crystal.

Figure 8 shows the spectrum of the X-ray emission from figure 6. The peak energy of the spectrum reflects the peak voltage between the crystals at the point of discharge, and in this case is 15-20 keV. The dielectric screening of the surface charge on each crystal has not been taken into account in equation 3, but it should enter as a multiplication factor to reduce the overall voltage. The screening factor is unlikely to substantially change the magnitude of the voltage. Accordingly, it is observed that the X-ray emission is commensurate with the measured charge.

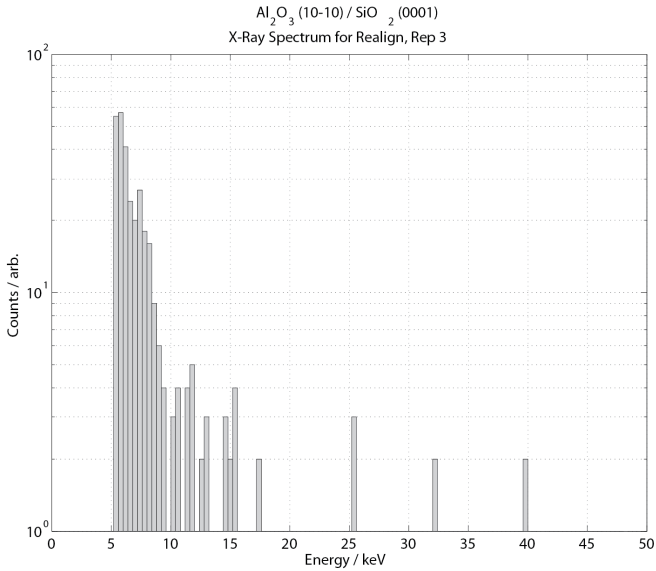


Fig. 8 Energy spectrum of X-rays observed in figure 6 that are implied by figure 5. The peak energy is ~ 15 keV, which is similar to the voltage inferred in figure 5 when dielectric screening is considered.

In all, despite large spread in the charging data, independent measurements of charge, discharge, and forces from fields are consistent with each other, suggesting that any spread in the data is in fact a result of the triboelectric interaction as performed. The system is ready to measure charging from surfaces that are less variable at the nanoscale.

IV. DISCUSSION

When considering any differences in charging for different crystal orientations, the full dataset is summarized in figure 9.

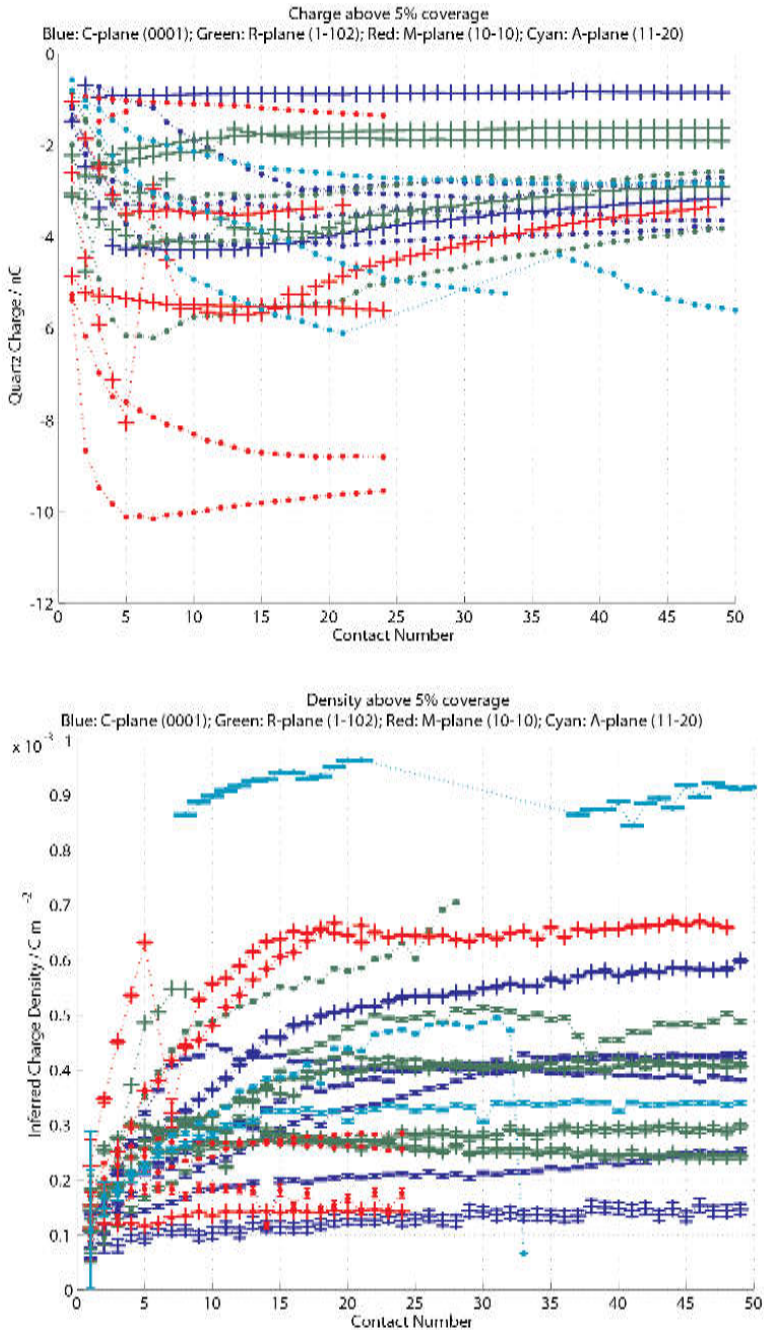


Fig. 9. Total charge and inferred density for sapphire A-(cyan), C-(blue), M-(red), and R-(green) planes when pressed against quartz. Only data where $A > 5\%$ is shown. No discernible correlation is seen between crystal orientation and strength of triboelectric interaction. All sapphire crystals charged positive.

While charging of sapphire against quartz is readily observed with consistent polarity, there is no discernible difference between the charging of any crystal orientation of sapphire. However, the spread of the data, even between two of the same orientation, is so large that the key parameter responsible for triboelectrification is clearly not being controlled within the experiment.

Without even considering contamination of the crystal surfaces, or surface reconstruction, the roughness of the surfaces ($R_a < 10 \text{ \AA}$) already poses a challenge for understanding the contact mechanics. Consider figure 10 that shows a cartoon of quartz approaching sapphire each with roughness $R_a \sim 10 \text{ \AA}$.

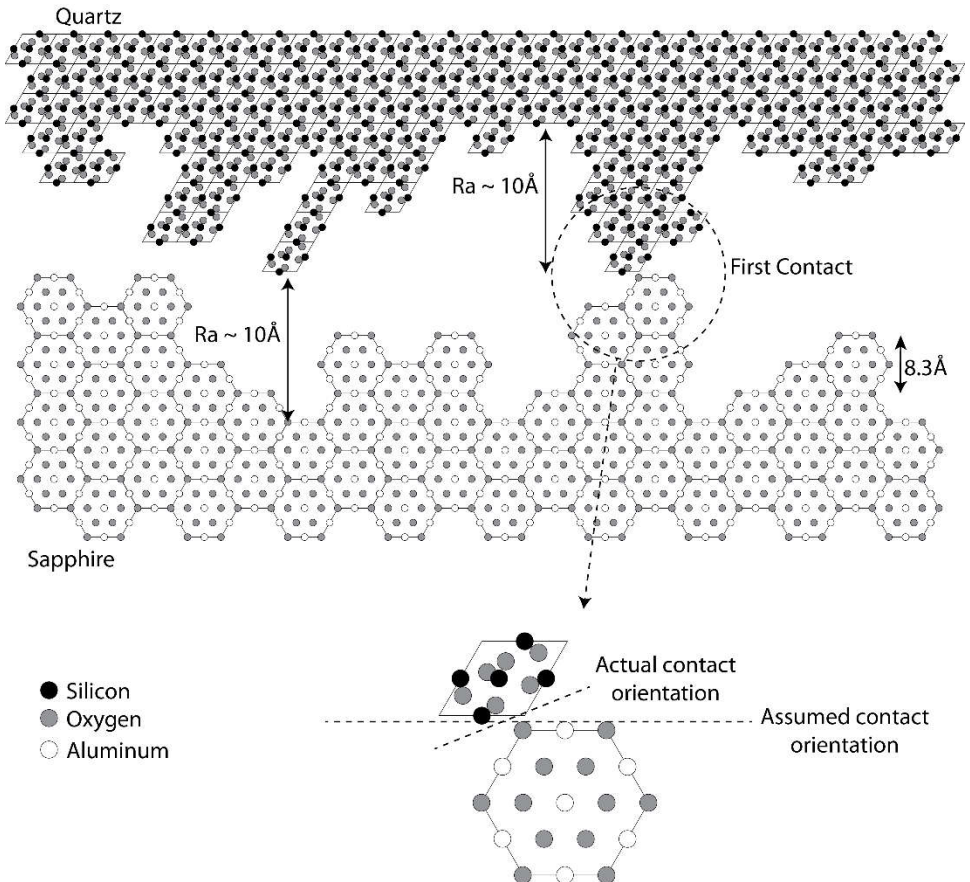


Fig. 10. Oriented quartz crystal approaching an oriented sapphire crystal, where both surfaces have roughness on the order typical of the crystals used in experiments presented here. The point of contact (circled) shows that instead of the crystals meeting perpendicular to their approach direction as expected, the roughness forces contact to occur at an arbitrary angle. This model doesn't even consider surface reconstruction or contamination, but the simple case can explain why no correlation is seen between the charging of different sapphire orientations.

While it may be expected that contact occurs along the polished planes, it immediately becomes clear that the presence of roughness can substantially change the orientation at

which the two crystals meet to exchange charge. Any structural cause for charge transfer can no longer be considered to come from the polished plane. As the crystal approach continues, more asperities contact at further different orientations, where contact electronics may well be different. To take the argument further, as the contact points yield and distort from stress and necessary reconstruction [22-25], there is no clear way to predict what the structure would even be at contact. Adding in the adsorption of contaminants such as a water layer further complicates the situation, as does inevitable rubbing on contact ($\sim 75 \mu\text{m}$ of slip [17]), and jitter in contact position. It becomes completely reasonable, then, that no correlation could be seen of the charging with crystal orientation; it is perhaps surprising that polarity remained consistent.

Controlling the bulk orientation was not influential enough in controlling surface charging. Even with consistent and independent measurements of charging, it would seem control of the crystal surfaces themselves requires more attention, as there is little to no control over the magnitude of the charging.

V. CONCLUSION

Data on the repeated contact charging of quartz and various crystal orientations of sapphire under vacuum conditions were presented. Sapphire will always charge positively against quartz, and the surface charges can accumulate to force a discharge in vacuum, which can even lead to X-ray emission. Despite having well-defined bulk structure, and actuation controlled down to the micron level, the sporadic nature of triboelectrification is still strongly prevalent. It is concluded that the material properties that direct triboelectrification are attributed to the surfaces of the crystals, control of which has not yet been sufficiently achieved with the apparatus.

Changes on the nanometer scale are manifesting at the macroscopic level in the measured triboelectrification and triboluminescence. It is perhaps remarkable that the polarity of the quartz/sapphire interaction was so robustly observed, and so some behavior is consistent in the face of substantial nanoscale variation.

Such conclusions are somewhat typical of a triboelectric experiment. Data seems largely spread due to changes at the surface beyond control of the experiment, and yet a consistent polarity pushes through, tempting a theory that doesn't have to consider the surface structure to exist.

VI. FURTHER DEVELOPMENT

More care must be taken to prepare and contact the surfaces under test. Reducing the roughness to a level where contact can be more predictable is desirable, and could be achieved with a modest number of asperities. Crystals may need to be etched and / or annealed *in situ* to achieve a smoother surface. Such surface treatment should also address the presence of surface contaminants.

To maintain cleanly prepared surfaces, a much stronger vacuum is advised to remove any ambient gas contact during experiment. Such a move would require more vacuum-compatible tools to run the experiment

Unintentional slip in contact and contact position jitter should also be addressed through improved sample mounting and solid mechanics.

VII. ACKNOWLEDGEMENTS

This study was funded by Tribogenics, Inc. Carlos Camara is thanked for useful discussions.

REFERENCES

- [1] P. O'Grady, *Thales of Miletus: the beginnings of Western science and philosophy*, Ashgate, 2002.
- [2] P. Iversen and D. J. Lacks, "A life of its own: The tenuous connection between Thales of Miletus and the study of electrostatic charging," *Journal of Electrostatics*, vol. 70, no. 3, pp. 309-311, 2012.
- [3] X. Shen, A. E. Wang, R. M. Sankaran and D. J. Lacks, "First-principles calculation of contact electrification and validation by experiment," *Journal of Electrostatics*, vol. 82, pp. 11-16, 2016.
- [4] R. Fu, X. Shen and D. J. Lacks, "First-Principles Study of the Charge Distributions in Water Confined between Dissimilar Surfaces and Implications in Regard to Contact Electrification," *The Journal of Physical Chemistry C*, vol. 121, no. 22, pp. 12345-12349, 2017.
- [5] W. B. Dapp and M. H. Müser, "Towards time-dependent, non-equilibrium charge-transfer force fields," *The European Physical Journal B*, vol. 86, no. 7, p. 337, 2013.
- [6] M. W. Williams, "Triboelectric charging of insulating polymers - some new perspectives," *AIP Advances*, vol. 2, no. 1, p. 010701, 2012.
- [7] R. G. Horn and D. T. Smith, "Contact Electrification and Adhesion Between Dissimilar Materials," *Science*, vol. 256, no. 5055, pp. 362-364, 1992.
- [8] B. N. J. Persson, O. Albohr, U. Tartaglino, A. I. Volokitin and E. Tosatti, "On the nature of surface roughness with application to contact mechanics, sealing, rubber friction and adhesion," *Journal of Physics: Condensed Matter*, vol. 17, no. 1, p. R1, 2005.
- [9] H. T. Baytekin, A. Z. Patashinski, M. Branicki, B. Baytekin, S. Soh and B. A. Grzybowski, "The Mosaic of Surface Charge in Contact Electrification," *Science*, vol. 333, no. 6040, pp. 308-312, 2011.
- [10] A. L. Collins, C. G. Camara, B. B. Naranjo, S. J. Putterman and J. R. Hird, "Charge localization on a polymer surface measured by triboelectrically induced x-ray emission," *Phys. Rev. B*, vol. 88, p. 064202, Aug 2013.
- [11] P. W. Tasker, "The stability of ionic crystal surfaces," *Journal of Physics C: Solid State Physics*, vol. 12, no. 22, p. 4977, 1979.
- [12] J. Tersoff, "Theory of semiconductor heterojunctions: The role of quantum dipoles," *Phys. Rev. B*, vol. 30, pp. 4874-4877, Oct 1984.
- [13] J. Tersoff, "Schottky barriers and semiconductor band structures," *Phys. Rev. B*, vol. 32, pp. 6968-6971, Nov 1985.
- [14] R. T. Tung, "Chemical Bonding and Fermi Level Pinning at Metal-Semiconductor Interfaces," *Phys. Rev. Lett.*, vol. 84, pp. 6078-6081, Jun 2000.
- [15] R. A. McKee, F. J. Walker, M. B. Nardelli, W. A. Shelton and G. M. Stocks, "The Interface Phase and the Schottky Barrier for a Crystalline Dielectric on Silicon," *Science*, vol. 300, no. 5626, pp. 1726-1730, 2003.
- [16] I. Siretanu, D. Ebeling, M. P. Andersson, S. S. Stipp, A. Philipse, M. C. Stuart, D. Van Den Ende and F. Mugele, "Direct observation of ionic structure at solid-liquid interfaces: a deep look into the Stern Layer," *Scientific reports*, vol. 4, p. 4956, 2014.
- [17] A. L. Collins, C. G. Camara, E. Van Cleve and S. J. Putterman, "Simultaneous measurement of triboelectrification and triboluminescence of crystalline materials," *Review of Scientific Instruments*, vol. 89, no. 1, p. 013901, 2018.
- [18] R. Massarczyk, P. Chu, C. Dugger, S. Elliott, K. Rielage and W. Xu, "Paschen's law studies in cold gases," *Journal of Instrumentation*, vol. 12, no. 06, p. P06019, 2017.
- [19] Y. Liao, "Practical Electron Microscopy and Database," GlobalSino, 2006. [Online]. Available: <http://www.globalsino.com/EM/page2591.html>. [Accessed 14 05 2018].

- [20] M. Leitner, "The α (low) Quartz Structure," 05 04 2000. [Online]. Available: <https://homepage.univie.ac.at/michael.leitner/lattice/struk/picts/sio2a.s.png>. [Accessed 14 05 2018].
- [21] R. N. Clarke, "Kaye & Laby Tables of Physical & Chemical Constants, 2.6.5 Dielectric properties of materials," National Physical Laboratory, 15 07 2015. [Online]. Available: http://www.kayelaby.npl.co.uk/general_physics/2_6/2_6_5.html. [Accessed 14 05 2018].
- [22] X.-G. Wang, A. Chaka and M. Scheffler, "Effect of the Environment on α -Al₂O₃ (0001) Surface Structures," *Phys. Rev. Lett.*, vol. 84, pp. 3650-3653, Apr 2000.
- [23] P. J. Eng, T. P. Trainor, G. E. Brown Jr., G. A. Waychunas, M. Newville, S. R. Sutton and M. L. Rivers, "Structure of the Hydrated α -Al₂O₃ (0001) Surface," *Science*, vol. 288, no. 5468, pp. 1029-1033, 2000.
- [24] C. Barth and M. Reichling, "Imaging the atomic arrangements on the high-temperature reconstructed α -Al₂O₃(0001) surface," *Nature*, vol. 414, p. 54, 2001.
- [25] S. E. Mason, C. R. Iccaman, T. P. Trainor and A. M. Chaka, "Density functional theory study of clean, hydrated, and defective alumina (1 $\bar{1}$ 02) surfaces," *Phys. Rev. B*, vol. 81, p. 125423, Mar 2010.